Muscle-like Supramolecular Polymers: Integrated Motion from Thousands of Molecular Machines

Guangyan Du, Emilie Moulin, Nicolas Jouault, Eric Buhler, Nicolas Giuseppone

Muscle-like Supramolecular Polymers - Integrated Motion from Thousands of Molecular Machines

Guangyan Du[1], Emilie Moulin[1], Nicolas Jouault[2†], Eric Buhler[2*] and Nicolas Giuseppone[1*]

Dedicated to Professor Sauveur Jean Candau

Endeavors in molecular nanosciences are increasingly directed towards the combination of structural and dynamic controls over hierarchical self-assemblies.[1, 2] These lines of research are often inspired by the complexity of living systems which associate molecular and supramolecular organization features in order to self-sustain and to evolve.[3] One of the most intriguing functional properties of living systems is their capacity to produce collective molecular motions and to amplify them by orders of magnitude. For instance, in muscular tissues, the coordinate movements of thousands of myosin heads lead to the gliding of thick myosin filaments along thin actin filaments which result in a cooperative contraction of the entire sarcomere. In that particular case, the individual shifts of the proteins take place in the 10 nm range whereas their integrated translation produces a 1 □m contraction of the sarcomeres, these latter being in turn coupled together, up to producing macroscopic motions.[4]

The chemical synthesis of artificial molecular machines (AMMs) is thus of central interest to mimic their biological counterparts with the hope of engineering dynamic microscopic devices and macroscopic functional materials by bottom-up approaches.[5-7] To date, a number of seminal works have been established regarding the design of individual AMMs which can produce internal motions such as *i*) translation in bistable single rotaxanes[8, 9] or on molecular tracks,[10] *ii*) scissor-like motions,[11] and *iii*) unidirectional circumrotation[12] (in multi-station catenanes) or rotation [13, 14] (around a central bond) in molecular motors driven far from equilibrium by light. In particular, going towards the design of synthetic molecular muscles, Sauvage and coworkers described the first unimolecular linear array capable of stretching and contracting on demand thanks to the action of a chemical stimulus.[15] In this approach, the authors used a double-threaded rotaxane (*i.e.* [*c*2]daisy chain, Figure 1A) in which both strings can glide along one another although locked together thanks to the rotaxane nature of the system. By introducing two kinds of specific ligands on the rotaxane axle, as well as a complementary ligand on the macrocyclic part, either contracted or extended forms can be simply obtained by exchanging the nature of the coordinated metal ions (Cu^{+} or Zn^{2+} in the present case). More recently, two important works published concomitantly by the groups of Stoddart[16, 17] and Grubbs[18] attempted to couple together pH-responsive [*c*2]daisy chain rotaxanes through “click” polymerization, with the aim of summing the contractions and extensions of the single machines along the polymer chains. However, and in both cases, the low degree of polymerization (average DP of 11 and 22, respectively) as well as the low solubility of the produced oligomers precluded the actuation and characterization of coupled translational motions towards mesoscopic scales. Thus, and although specifically targeted for a long time by the scientific community,[19] the linear amplification of muscle-like translational molecular motions by orders of magnitude has not been yet demonstrated experimentally.

[*] [1]G. Du, Dr. E. Moulin, Prof. Dr. N. Giuseppone
SAMS research group – University of Strasbourg – Institut Charles Sadron, CNRS, 23 rue du Loess, BP 84047, 67034 Strasbourg Cedex 2, France, Homepage: http://www-ics.u-strasbg.fr/sams.
E-mail: giuseppone@unistra.fr
Homepage: http://www-ics.u-strasbg.fr/sams/

[2]Dr. N. Jouault, Prof. Dr. E. Buhler
Matière et Systèmes Complexes (MSC) Laboratory, University of Paris Diderot – Paris VII, UMR 7057, Bâtiment Condorcet, 75205 Paris Cedex 13, France.
E-mail: eric.buhler@paris7.jussieu.fr

† Current address: Columbia University, Department of Chemical Engineering, 500W 120th, New York, NY 10027, United States.

[**] The research leading to these results has received funding from the European Research Council under the European Community's Seventh Framework Program (FP7/2007-2013) / ERC Starting Grant agreement n°257099 (N.G.). We wish to thank the CNRS, the icFRC, and the University of Strasbourg for financial supports, and the Laboratoire Léon Brillouin (LLB, CEA, Saclay, France) for beamtime allocation. This work was also supported by a post-doctoral fellowship from the Agence Nationale de la Recherche (ANR-09-BLAN-034-02) (NJ), and a doctoral fellowship from the Chinese Scholarship Council (G.D.).

Here we describe the design of a pH-triggered muscle-like system in which tailored bistable [*c*2]daisy chain rotaxanes are combined linearly by taking advantage of a metallo-supramolecular polymerization process (Figure 1B). Our approach leads to sufficiently long and soluble polymer chains to measure micrometric changes of their contour length upon synchronization of thousands of contractions and extensions. To this end, targeted monomer **1** has been synthesized by a 13-step pathway in its longest sequence starting from commercially available 4-bromobenzyl alcohol (Scheme 1). After acetylation of the alcohol, introduction of TMS-protected acetylene catalyzed by palladium and subsequent desilylation, compound **4** was engaged in a copper-free Sonogashira coupling with terpyridine triflate **5** to yield acetate **6**. The efficient three-step sequence to introduce the azide group affords compound **7** which can then be readily engaged in a Huisgen cycloaddition catalyzed by copper(I) with the already described bis-alkyne pseudorotaxane **8**.[20a] The final steps of this sequence consist in the protection of the terpyridine with copper triflate prior to selective methylation of triazole **9** with iodomethane. The removing of coordinated copper with EDTA followed by the exchange between iodide and hexafluorophosphate counterions gives the desired [*c*2]daisy chain **1** with an excellent overall yield of 21%. The bistable nature of this rotaxane is provided by the two binding sites on its axle, *i.e.* the secondary ammonium and the triazolium, which are known in the literature[20b-e] to present different binding constants with the dibenzo-24-crown-8 ether. In its protonated form, the ammonium binds to the macrocycle (extended $\mathbf{1}^{ext}$), whereas in its deprotonated one the crown ether moves to the triazolium site (contracted $\mathbf{1}^{cont}$), as confirmed by ^{1}H NMR titrations in both directions using either trifluoroacetic acid or sodium hydroxide (Figure S1 in SI).

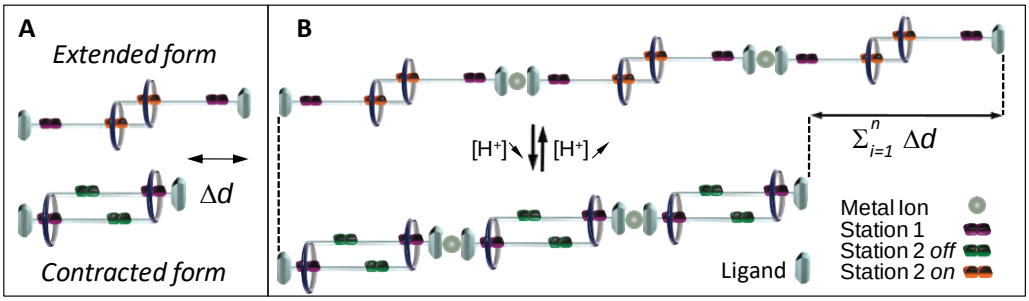

Figure 1. (**A**) General functioning principle of a bistable [*c*2]daisy chain rotaxane. The double threaded structure is kept interlocked by the presence of two gray stoppers at the end of each axle. The extended and contracted forms are selectively obtained by playing on the differential binding constants of the macrocycles with the two stations located on the axle. (**B**) The supramolecular polymer of this study is composed of [*c*2]daisy chains in which the stoppers can also bind to metal ions and produce coordination polymers. In this case, station 2 can be switched on and off by pH modulations, thus changing its relative binding affinity for the macrocycle compared to station 1. The integrated translational motion of the supramolecular polymer chain is the product of the individual contractions and extensions of each molecular machine by the degree of polymerization.

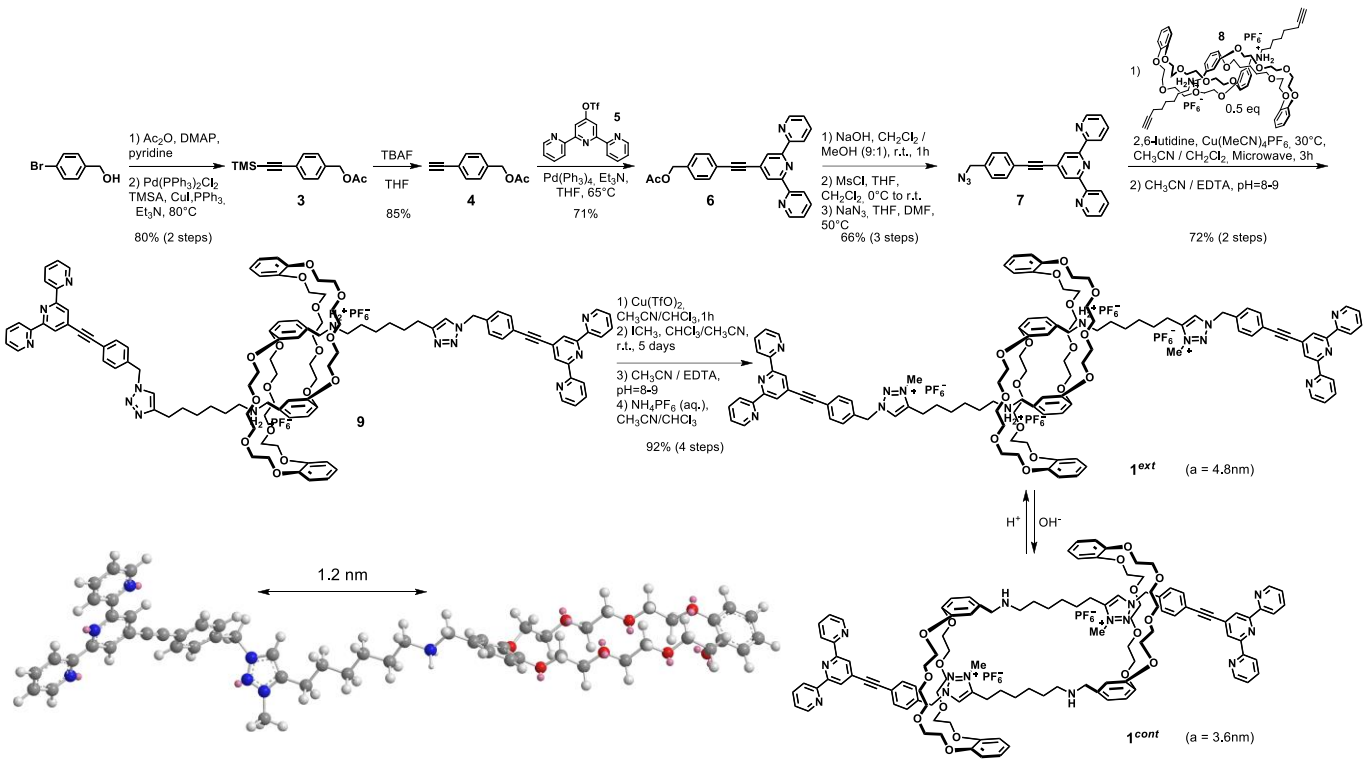

Scheme 1. Synthetic pathway for building monomeric molecular machine **1**. In this [*c*2]daisy chain terminated by two bulky terpyridine ligands, the dibenzo-24-crown-8 ether can bind either to station 1 (triazolium) or to station 2 (ammonium); these latter can be switched off and on by deprotonation/reprotonation, leading respectively to a contracted form **1**^{cont} or to an extended one **1**^{ext} depending on the pH of the solution. The lengths of **1**^{ext} (a=4.8 nm) and **1**^{cont} (a=3.6 nm), as well as the distance between the two stations (□d=1.2 nm), have been determined by molecular modelling.

We then turned to the supramolecular polymerizations of **1**^{cont} and **1**^{ext} using one equivalent of either $Zn(OTf)_2$ or $FeCl_2$ as metal ions in a $CDCl_3/CD_3CN$ 1:1 solution ([**1**] = 10 mM). As expected, the ^1H NMR spectra of the four resulting products (namely **Zn1**^{cont}, **Zn1**^{ext}, **Fe1**^{cont}, and **Fe1**^{ext}) were too broad to be informative although strong shifts could be identified in the terpyridine region, indicating a probable binding of the metal ions. This coordination was however unambiguously confirmed by UV-Vis analyzes (Figure S2 in SI) in which the appearing band around 340 nm in the four solutions, as well as the new charge transfer band at 580 nm for **Fe1**^{cont} and **Fe1**^{ext} are in agreement with the formation of the bis-terpyridine complexes.[21, 22]

To probe further the length of the expected supramolecular polymers, as well as their conformation, we have combined a series of light and small-angle neutron scattering (SANS) experiments and extracted key structural parameters grouped in Table 1. SANS is the most powerful method to determine characteristic sizes and shapes of objects in solution over the range of 1-300 nm. The scattering pattern for a 10 mM solution of **Zn1**^{cont} that is below the overlap concentration is displayed in Figure 2A. The product $M_wP(q)$ as a function of the scattered wave-vector q[23] has been obtained by coupling low-q static light scattering (SLS) and SANS measurements, where M_w is the weight-average molecular weight of the scattered species and P(q) the form factor (see SI). The scattering curve exhibits an overall behavior characterized by the following sequence: *i*) an onset of a smooth variation analogous to a Guinier regime at very low-q, associated with the finite size and mass of the objects; *ii*) a low-q regime in which the q-dependence of the data can be described by a power law with exponent close to -2, like in Gaussian coils; *iii*) a q^{-1} domain at intermediate q characteristic of a rigid rod-like behavior for distances smaller than the persistence length L_p, followed by *iv*) another Guinier regime associated with the cross-section of the polymers. This ensemble of variations is characteristic of worm-like chain behavior.[24] In such case, one usually represents scattering data by a "Holtzer plot"[25] of the product $M_wP(q)$□q as a function of q as is shown in Figure 2B, which directly demonstrates the crossover from a rigid rod-like to a coil-like behavior at a length scale of L_p.

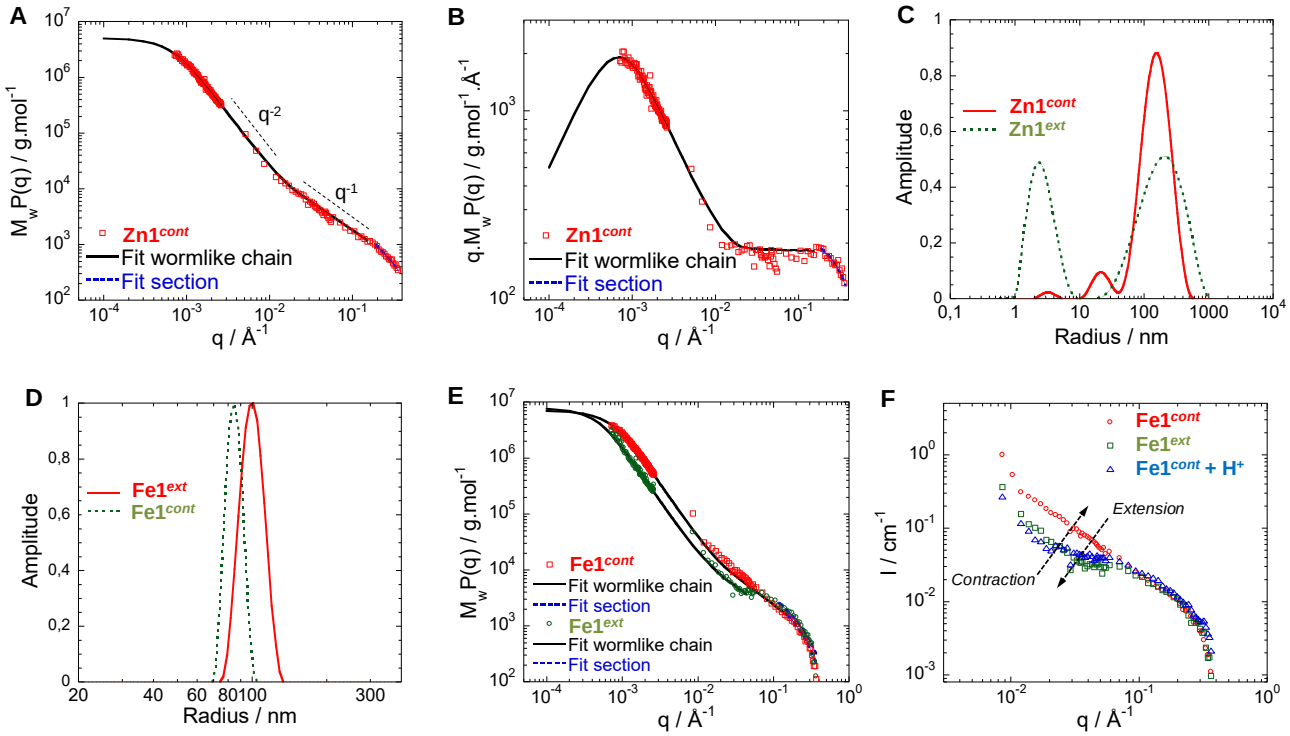

Figure 2. (**A**) Log-Log plot of combined SLS and SANS measurements for a solution of **Zn1**^{cont} (10 mM in 1:1 $CDCl_3/CD_3CN$ at T=20°C); (**B**) corresponding Holtzer plot. The continuous line represents the data fit by the wormlike chain model (eq. S10 in SI) and the dashed line represents the data fit at high-q by a Guinier expression for the form factor of the section (eq. S11 in SI). (**C**) Distribution of the scattering intensity with the hydrodynamic radii (R_H) obtained by applying the Contin method to our data at □=90° for Zn-based supramolecular polymers and (**D**) for Fe-based supramolecular polymers. (**E**) SLS and SANS data for **Fe1**^{ext} and **Fe1**^{cont} (10 mM in 1:1 $CDCl_3/CD_3CN$ at T=20°C). The continuous lines represent the best fit of the data by a wormlike chain model (eq. S10 in SI) and the dashed line represents the data fit at high-q by a Guinier expression for the form factor of the cross-section (eq. S11 in SI). (**F**) SANS only showing the effect of *in situ* protonation (2 equiv. of CF_3CO_2D) starting from **Fe1**^{cont} and leading to **Fe1**^{ext} as compared with the reference of **Fe1**^{ext} polymerized from already extended monomer.

The ensemble of variations shown in Figure 2A,B can be considered as a form factor and fitted satisfactorily by a wormlike chain model, yielding persistence length L_p=15.5±1.6 nm, linear mass density $M_L=M_w/L_c$ =585±110 g/mol/nm, and contour length L_c=8854±900 nm. From the data at q=0, one obtains a polymerization degree (DP) of 1967±190, a value in agreement with the theoretical one expected from the thermodynamic stability of the complex at this concentration. The level of the intermediate q^{-1}-regime is controlled by the M_L value, which is in excellent agreement with that of a single-strand polymer chain (linear mass density of deprotonated monomer **1*cont*** is m/a=2632/3.6=731 g/mol/nm, where m and a represent the mass and the length of a monomer unit respectively (Figure S3 and Table S1 in SI)). The high-q data has been fitted by a Guinier expression for the form factor of the polymer section, determining the cross-section, S=1.42±0.15 nm^2, and the radius of gyration of the cross-section, R_c=0.3±0.03 nm, values in agreement with monomers section.

As shown by the dynamic light scattering (DLS) experiments presented in Figure 2C, **Zn1*ext*** samples present a partial depolymerization. The size distribution obtained by applying the Contin analysis to our data shows two populations, one around 2-3 nm corresponding to monomers and another one around 200 nm corresponding to polymers. The hydrodynamic radius of the **Zn1*cont*** sample obtained from extrapolation of the data at zero-q is R_H=206±20 nm. This observation was confirmed by starting with the preformed polymer and by adding increasing amounts of trifluoroacetic acid, revealing a competition between protonation and coordination with the zinc ions. To avoid such drawback, we turned to Fe(II) ions as coordination metal which is known to bind even more strongly with terpyridine ligands (log□=20.9 M^{-2} in water).[26] Gratifyingly, DLS measurements performed on iron systems indicate the presence of a single polymer population for all deprotonated and protonated samples at various temperatures (Figure 2D and Figure S4 in SI). We have determined after extrapolation of the data at q=0 a R_H=167±17 nm for **Fe1*cont*** and a R_H=189±19 nm for **Fe1*ext***.

Table 1.Characteristic structural parameters obtained from the DLS, SLS, and SANS experiments for polymers **Zn1*cont***, **Fe1*cont***, and **Fe1*ext***. (**A**) Theoretical values; (**B**) Experimental parameters obtained from the fitting procedure. According to the optimization of the fitting procedures, the calculation of the contrast and the measurement of the monomer density (see SI), we estimate an absolute error within 10% on the characteristic structural parameters of Table 1B.

(**A**)

	M° (g/mol)	**a_{theo} (nm)**	**M_{Ltheo} (g/mol/nm)**	□
Zn1*cont*	2334	3.6	648	0.0202
Fe1*cont*	2395	3.6	665	0.0184
Fe1*ext*	2687	4.8	559	0.0190

(**B**)

	$M_{w\ fit}$ (x10⁶ g/mol)	**DP**	**L_c (nm)**	**L_{ctheo}[A] (nm)**	**$M_{l\ exp}$(g/mol/nm)**
Zn1*cont*	5.179	1967	8854	8261	585
Fe1*cont*	7.030	2937	9398	10573	748
Fe1*ext*	7.890	2937	15861	14097	498

[A] $L_{ctheo}=DP*a_{theo}$

	L_p (nm)	**$R_{g\ Benoît-Doty}$ (nm)**	**a_{exp}(nm)**	**R_c (nm)**	**S (nm²)**	**R_h (nm)**
Zn1*cont*	15.5	213	4.5	0.30	1.412	206
Fe1*cont*	12.8	200	3.2	0.45	1.791	167
Fe1*ext*	17.6	305	5.4	0.40	1.596	189

The scattering patterns of **Fe1*cont*** and **Fe1*ext*** in 10 mM solutions are displayed in Figure 2E and at various temperatures in Figure S5 in SI. Both samples exhibit the same wormlike-chain behavior, characterized by the sequence described above for **Zn1*cont***. Scattering variations are fitted satisfactorily by the wormlike-chain model and one obtains respectively L_p=12.8±1.3 nm, M_L=748±150 g/mol/nm, L_c=9398±1000 nm, and DP=2937±290 for **Fe1*cont*** and L_p=17.6±1.8 nm, M_L=498±100 g/mol/nm,

L_c=15861±1500 nm, and DP=2937±290 for **Fe1**^{ext}. The contraction-extension process is clearly demonstrated by these results as for the **Fe1**^{ext} sample we observe *i*) an increase of the contour length of the chain, and *ii*) a reduction of the linear density. The values of the experimental linear mass densities are in agreement with that calculated for a single-strand contracted chain (m/a=665 g/mol/nm) and for a single-strand extended chain (m/a=559 g/mol/nm). Cross-section dimensions for both iron samples correspond to that of a monomer section, confirming that no lateral aggregation occurs: R_c=0.42±0.04 nm and S=1.7±0.15 nm^2. We have also checked by using SANS the effect of the *in situ* protonation of **Fe1**^{cont} which confirms the extension of the supramolecular polymer because, in the q^{-1} regime, the intensity of **Fe1**^{cont} + H^+ overlaps with the one measured for the sample **Fe1**^{ext} prepared by the supramolecular polymerization from already protonated monomer **1**^{ext} (Figure 2F).

This work shows, through a number of experimental evidences, that the coupling of thousands of molecular machines along a single polymer chain provides a pathway to integrate their single motions at mesoscale. The key features of the present system rests on a very efficient metallo-supramolecular polymerization of highly functional and bistable [c2]daisy chains which produce perfect worm-like chains. This crucial experimental aspect allows a clear and precise determination of the occurring one-dimensional contraction process, and avoids parasitic effects that would be necessarily brought by cross-chain interactions. By looking at **Fe1**^{ext} and **Fe1**^{cont}, the shift between the two SANS curves is the signature of the relative change in linear mass density between the two samples and one can quantify it with an excellent precision (ΔM_L=250±25 g/mol/nm). This local change of the polymer chain is directly correlated with the global change of the polymer contour length (ΔL_c=6.4±0.7 μm; a value which is, by analogy, in the range of the contraction observed in sarcomeres). The measured effect is in good agreement with the expected theoretical value based on the distance between the two stations and on the degree of polymerization. They also perfectly fit with the experimental SANS values measured on both monomers as references. Thus, this amplification by four orders of magnitude of the mechanical output of thousands of molecular machines linked within a single-strand macromolecular chain, going from the low nanometer scale to the ten of micrometers, is accessible by combining molecular synthesis, supramolecular engineering, and polymerization processes. The next challenge to access macroscopic responses will consist in playing with the persistence length of these single chain polymers, and in bundling and orienting them in stiffer fibers, just as myofibrils do in muscles.

Received: ((will be filled in by the editorial staff))
Published online on ((will be filled in by the editorial staff))

Keywords: Molecular machines · Supramolecular polymers · Responsive materials · Nanotechnology

[1] J.-M. Lehn, *Science* **2002**, *295*, 2400-2403.
[2] G. M. Whitesides, B. Grzybowski, *Science* **2002**, *295*, 2418-2421.
[3] S. Mann, *Angew. Chem. Int. Ed.* **2008**,*47*, 5306-5320;*Angew. Chem.* **2008**, *120*, 5386-5401.
[4] J. L. Krans, *Nature Education* **2010**, *3*, 66.
[5] K. Kinbara, T. Aida, *Chem. Rev.* **2005**, *105*, 1377-1400.
[6] E. R. Kay, D. A. Leigh, F. Zerbetto, *Angew. Chem. Int. Ed.* **2007**, *46*, 72-191; *Angew. Chem.* **2007**, *119*, 72-196.
[7] L. Fang, M. A. Olson, D. Benítez, E. Tkatchouk, W. A. Goddard III, J. F. Stoddart,*Chem. Soc. Rev.* **2010**, *39*, 17-29.
[8] R. A. Bissell, E. Córdova, A. E. Kaifer, J. F. Stoddart, *Nature* **1994**, *369*, 133-137.
[9] B. K. Juluri, A. S. Kumar, Y. Liu, T. Ye, Y.-W. Yang, A. H. Flood, L. Fang, J. F. Stoddart, P. S. Weiss, T. J. Huang, *ACS Nano* **2009**, *3*, 291-300.
[10] M. von Delius, E. M. Geertsema, D. A. Leigh, *Nature Chem.* **2010**, *2*, 96-101.
[11] T. Muraoka, K. Kinbara, Y. Kobayashi, T. Aida, *J. Am. Chem. Soc.* **2003**, *125*, 5612-5613.
[12] D. A. Leigh, J. K. Y. Wong, F. Dehez, F. Zerbetto, *Nature* **2003**, *424*, 174-179.
[13] N. Koumura, R. W. J. Zijistra, R. A. Van Delden, N. Harada, B. L. Feringa, *Nature* **1999**, *401*, 152-155.
[14] T. R. Kelly, H. De Silva, R. A. Silva, *Nature* **1999**, *401*, 150-152.
[15] M. C. Jiménez, C. Dietrich-Buchecker, J.-P.Sauvage, *Angew. Chem. Int. Ed.* **2000**, *39*, 3284-3287; *Angew. Chem.* **2000**, *112*, 3422-3425.
[16] L. Fang, M. Hmadeh, J. Wu, M. A. Olson, J. M. Spruell, A. Trabolsi, Y.-W.Yang, M. Elhabiri, A.-M. Albrecht-Gary, J. F. Stoddart, *J. Am. Chem. Soc.* **2009**, *131*, 7126-7134.
[17] L. Fang, M. Hmadeh, A. Trabolsi, M. Elhabiri, A.-M.Albrecht-Gary, J. F. Stoddart, *J. Mater. Chem.* **2010**, *20*, 3422-3430.

[18] P. G. Clark, M. W. Day, R. H. Grubbs, *J. Am. Chem. Soc.* **2009**, *131*, 13631-13633.

[19] B. L. Feringa, *Nature* **2000**, *408*, 151-154.

[20] a) F. Coutrot, C. Romuald, E. Busseron, *Org. Lett.* **2008**, *10*, 3741-3744; b) F. Coutrot, E. Busseron, *Chem. Eur. J.* **2008**, *14*, 4784–4787; c) C. Romuald, A. Ardá, C. Clavel, J. Jiménez-Barbero, F. Coutrot, *Chem. Sci.* **2012**, *3*, 1851-1857; d) C. Romuald, E. Busseron, F. Coutrot, *J. Org. Chem.* **2010**, *75*, 6516-6531; e) Y. Jiang, J.-B. Guo, C.-F. Chen, *Org. Lett.* **2010**, *12*, 4248-4251.

[21] S.-C. Yu, C.-C. Kwok, W.-K. Chan, C.-M. Che, *Adv. Mater.* **2003**, *15*, 1643-1647.

[22] H. Hofmeier, R. Hoogenboom, M. E. L. Wouters, U. S. Schubert, *J. Am. Chem. Soc.* **2005**, *127*, 2913-2921.

[23] J. Appell, G. Porte, E. Buhler, *J. Phys. Chem.* **2005**, *109*, 13186-13194.

[24] E. Buhler, F. Boué, *Eur. Phys. J. E* **2003**, *10*, 89-92.

[25] M. Rawiso, *J. Phys. IV* **1999**, *9* (Pr1), 147-195.

[26] A. E. Martell, R. M. Smith, *Critical Stability Constants*, Plenum Press, New York, **1974.**